DOI: 10.1002/adfm.201702225
**Article type: Full Paper**

# Hybrid photonic nanostructures by in vivo incorporation of an organic fluorophore into diatom algae

*Roberta Ragni, Francesco Scotognella, Danilo Vona, Luca Moretti, Emiliano Altamura, Giacomo Ceccone, Dora Mehn, Stefania R. Cicco, Fabio Palumbo, Guglielmo Lanzani* and Gianluca M. Farinola**

Dr. R. Ragni, Dr. D. Vona, Dr. E. Altamura, Prof. G. M. Farinola
Dipartimento di Chimica, Università degli Studi di Bari "Aldo Moro", via Orabona 4, I-70126 Bari, Italy
E-mail: gianlucamaria.farinola@uniba.it
Dr. F. Scotognella, Dr. L. Moretti
Dipartimento di Fisica, Politecnico di Milano, piazza Leonardo da Vinci 32, 20133 Milano, Italy
Dr. G. Ceccone, Dr. D. Mehn
European Commission, Directorate General Joint Research Centre, Directorate F-Health, Consumers and Reference Materials, Consumer Products Safety Unit, via E. Fermi 2749, TP125, I21027, Ispra, Italy
Dr. S. R. Cicco
CNR-ICCOM-Bari, Dipartimento di Chimica, via Orabona 4, I-70126 Bari, Italy
Dr. F. Palumbo
CNR-NANOTECH-Bari, Dipartimento di Chimica, via Orabona 4, I-70126 Bari, Italy
Prof. G. Lanzani
Dipartimento di Fisica, Politecnico di Milano, piazza Leonardo da Vinci 32, Istituto Italiano di Tecnologia, Center for Nano Science and Technology, via Pascoli 70/3, 20133 Milano, Italy

Keywords: photonic crystals, diatoms, biosilica, photoluminescence, molecular emitters

Biotechnological processes harnessing living organisms' metabolism are low-cost routes to nanostructured materials for applications in photonics, electronics and nanomedicine. In the pursuit of photonic biohybrids, diatoms microalgae are attractive given the properties of the porous micro-to-nanoscale structures of the biosilica shells (frustules) they produce. Our investigations have focused on *in vivo* incorporation of tailored molecular fluorophores into

the frustules of *Thalassiosira weissflogii* diatoms, using a procedure that paves the way for easy biotechnological production of photonic nanostructures. The procedure ensures uniform staining of shells in the treated culture and permits the resulting biohybrid photonic nanostructures to be isolated with no damage to the dye and periodic biosilica network. Significantly, this approach ensures that light emission from the dye embedded in the isolated biohybrid silica is modulated by the silica's nanostructure, whereas no modulation of photoluminescence is observed upon grafting the fluorophore onto frustules by an *in vitro* approach based on surface chemistry. These results pave the way to the possibility of easy production of photonic nanostructures with tuneable properties by simple feeding the diatoms algae with tailored photoactive molecules.

## 1. Introduction

Some living organisms have optimized, in billion years of natural evolution, their ability to generate photoactive components essential for their survival, with complex macro- to nanoscale structures and highly reproducible features. Nanostructured biomaterials represent a very promising alternative to the synthetic counterparts, due to great advantages for scalability, low production costs and high reproducibility of their hierarchical nanostructures, whose levels of symmetry and complexity can be well far beyond those achieved by the best technologies available thus far.

Among living organisms that generate nanostructured photoactive components, diatoms are very attractive. They are a large and prolific class of single cell photosynthetic microalgae (Bacillariophyta), whose mesoporous biomineralized silica shells, called frustules, encase the organic protoplasm.[1] Decorated with quasi-periodic three-dimensional hierarchical patterns of pores, on both the nano- and microscale, frustules have a pill-box like structure consisting of two valves, the epitheca and the hypotheca, connected by lateral rings, known as girdles, which give the structure its flexibility.[2] Pore size varies from 50 nm to more than one micron,

while cell size ranges from microns to millimetres depending on the species. Various theories have been put forward about what frustules are intended to do, from physically protecting the protoplasm from the surrounding environment,[3] controlling nutrient uptake and cell secretion,[4] to assisting in light collection.[5] Given the existence of the enormous number of diatom species (more than $2 \cdot 10^5$), each with characteristic biosilica patterns and the ease with which they can be farmed, diatoms' biosilica shells have, for some time now, been eyed up as a low-cost source of mesoporous biomaterials to be used in a variety of applications, ranging from drug delivery,[6,7] semiconductor production,[8] to light focusing and filtering in optics and photonics.[9,10] To date, studies on photonics have mostly been carried out on bare frustules extracted from living diatoms. Due to the ordered periodic patterns of high and low refractive index found in the mesoporous frustule nanoarchitecture of the *Coscinodiscus granii* diatom, both bare valve and girdle components have been early regarded as slab waveguide photonic crystals by Furhmann *et al.*[10a] Bare valves of the *Coscinodiscus wailesii* algal species have been also recently demonstrated by De Stefano *et al.* to focus light and confine it in a train of hotspots whose position, along the optical axis, changes varying wavelength.[10b,c] Kieu *et al.* also observed that radiating local areas of *Coscinodiscus wailesii* valves with a white laser source, a different transmission and diffraction of single wavelengths occurs as a result of changes in the spacing of valve pores.[10d] These features disclose possible application of single valves as micro-monochromator elements, optical micro-filters or micro-lenses.

Frustules chemically modified with organic dyes have seldom been investigated for their optical properties thus far. On the other hand, organic dyes have commonly been used as bioimaging tools in investigations into the life cycle of diatoms and, in particular, the biomineralization mechanism which creates their frustules.[11] A step forward was taken in a study by Furhmann *et al.* in 2012 on the valves of *Coscinodiscus granii* and *Coscinodiscus*

*wailesii* diatoms isolated after *in vivo* staining with rhodamine dyes,[12] which showed that the emission colour of the stained biosilica differs from that of the molecular dye in solution.

All this research has successfully focused on dyes as staining agents. However, when we switch perspective, and promote the applicative goals of staining as a route for materials production, the focus changes from perfecting technique to rethinking the steps that need to be undertaken to achieve such goals. One aspect of this rethinking is to work out a flexible but straightforward route to creating chemically modified biosilica as nanomaterials for applications in photonics. Functionalization of the silica's nanostructured shells with organic fluorophores that harnesses *in vivo* biomineralization is one way of doing this. The overall process leads to the biotechnological production of photonic materials whose properties derive from the combination of the frustule's photonic structure and the incorporated dye's optical properties. Crucially, *in vivo* addition of a tailored dye to the diatom culture functionalizes the silica skeleton deep down. It goes right to the core, giving rise to concerted interaction between the dye's fluorophore emission and the frustule's photonic structure. On the contrary, when functionalization is limited to the surface of isolated frustules, the dye's emission spectrum remains almost unchanged.

Our approach to the farming of biohybrid photonic micro/nano structures is based on the *in vivo* staining of the *Thalassiosira weissflogii*'s frustules with a functional molecular fluorofore (PE-Syl in **Figure 1**). This is followed by the removal of the organic protoplasm using an acidic-oxidative protocol that leaves both the periodicity of luminescent biosilica structures and the dye's molecular structure unaffected. Light transmission spectroscopy in different areas of valves and girdles, backed up by theoretical modelling, shows that the light transmitted depends on pore patterns in the different frustule regions of this diatom. The pore pattern modulates the dye photoluminescence as an effect of the interaction of the light emitted with the photonic structure of biosilica. The dye's emission is measured by light-emission spectroscopy of a dye-stained biosilica film and by confocal microscopy of local

areas of valves and girdles. To the best of our knowledge, such a spatially-resolved spectroscopic study of the dye stained biosilica from diatoms has not been previously reported in the literature and it would appear to be an important preliminary step as regards furthering applications in photonics of this luminescent nanostructured material.

## 2. Results and Discussion

### 2.1. Chemical design of the dye and *in vivo* feeding of diatoms.

Three fluorophores with a phenyleneethynylene conjugated backbone (PE-Syl, PE-acid and PE-amide in **Figure 1**) but different functional groups (triethoxysilyl, carboxyl, amide, respectively) were synthesized and investigated for frustule staining.

The phenyleneethynylene backbone was selected because of its high photoluminescence efficiency, low cytotoxicity and good photochemical stability,[13] as also shown in our previous study on selective staining of both living and fixed cell membranes.[14] We also recently demonstrated that phenyleneethynylene dyes' structure can be covalently conjugated with a transmembrane photosynthetic enzyme without denaturation and that these dyes can be used to enhance the light harvesting ability of this photoenzyme.[15] The unhindered linear molecular structure and moderate molecular weight (below 1KDa) were expected to facilitate the uptake of these dyes into the diatom silica deposition vesicles where the biosilicification process takes place. Alkoxy substituents were introduced to shift the photoluminescence batochromically from the UV to the blue region of the visible spectrum so as to detect fluorophore emission by fluorescence microscopy of diatoms during *in vivo* staining, and avoid overlap with the red photoluminescence of chloroplasts.

The triethoxysilyl group of PE-Syl was introduced to permit covalent bonding of the PE taken up by the cells to the biosilica during the biosilicification process, which is normally based on orthosilicic acid $Si(OH)_4$ as the inorganic silicon source.[16] Moreover, the propyl spacer

between the nitrogen atom and the silyl group may favor the involvement of PE-Syl into the biomineralization process, being similar to the amino propyl monomeric units of the natural long chain polyamines (LCPAs) involved in the silica biomineralization process of living diatoms.[16b,c]

PE-amide and PE-acid were used as two reference systems.

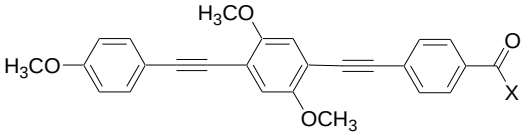


**PE-Syl** ; X= NH $Si(OEt)_3$

**PE-amide** ; X= NH

**PE-acid** ; X= OH

**Figure 1.** Chemical structures of phenyleneethynylene dyes

For the *in vivo* staining experiments, dimethylsulphoxide solutions of the dyes (120 µL, 0.03M) were added to three samples of living *Thalassiosira weissflogii* diatoms cultured as described in the Supporting Information (see S2) and suspended in a Guillard's medium enriched with glucose and sodium metasilicate (see Experimental Section). The amount of dye added was the minimum that allowed fluorescence microscopy observation of the dye's blue photoluminescence during and after *in vivo* staining. Good dispersion in the aqueous sodium methasilicate-enriched culture medium was observed for PE-Syl, while PE-acid and PE-amide immediately precipitated from the aqueous solution.

The biosilica staining was detected by recording fluorescence microscopy images of living diatoms at 30 min, 90 min, 8 h and 24 h after the addition of PE-Syl (Figure 2, lines i, ii, iii, iv respectively). The images taken at 24 h show that the dye does not physiologically damage diatoms and is incorporated into both valves in a frustule, which are being formed in the cell division step, that usually requires at least 6 h, during which two new hypotheca valves are created. Images were recorded using a TRITC filter, a DAPI filter, and a merge mode of both channels (Figure 2, columns a, b, c respectively). In particular, the TRITC filter allowed us to

monitor cell viability. It revealed autofluorescence of the red-emitting chloroplasts of the living diatoms, whereas the DAPI filter detected PE-Syl blue emission.

Images recorded after 30 min showed intense red chloroplast photoluminescence (Figure 2ai) and weak incorporation of PE-Syl in the endocellular areas with no specific compartmentalization (Figure 2bi and 2ci). At 90 min, diatoms were still viable (Figure 2aii); cell division was observed (Figure 2bii) and the blue dye emission was more evident inside the cells (Figure 2cii). After 8 h, the diatoms took on the appearance of bright blue luminescent micro-pills (Figure 2biii, 2ciii) containing red-emitting chloroplasts (Figure 2aiii), indicating that the PE-Syl had been incorporated into the biosilica shells. The typical box-like shape of frustules during division (where the valves remained linked by a quasi-connectival system) was also visible (Figure 2biii). After 24 hours, the appearance of bright blue fluorescent spots surrounding red chloroplasts may have been due to the accumulation of the dye in the silica deposition vesicles (Figure 2civ). The blue staining of cell biosilica walls was homogenous (Figure 2civ); the stained diatoms had a robust chloroplast auto-organization (Figure 2aiv) and were still capable of reproduction.

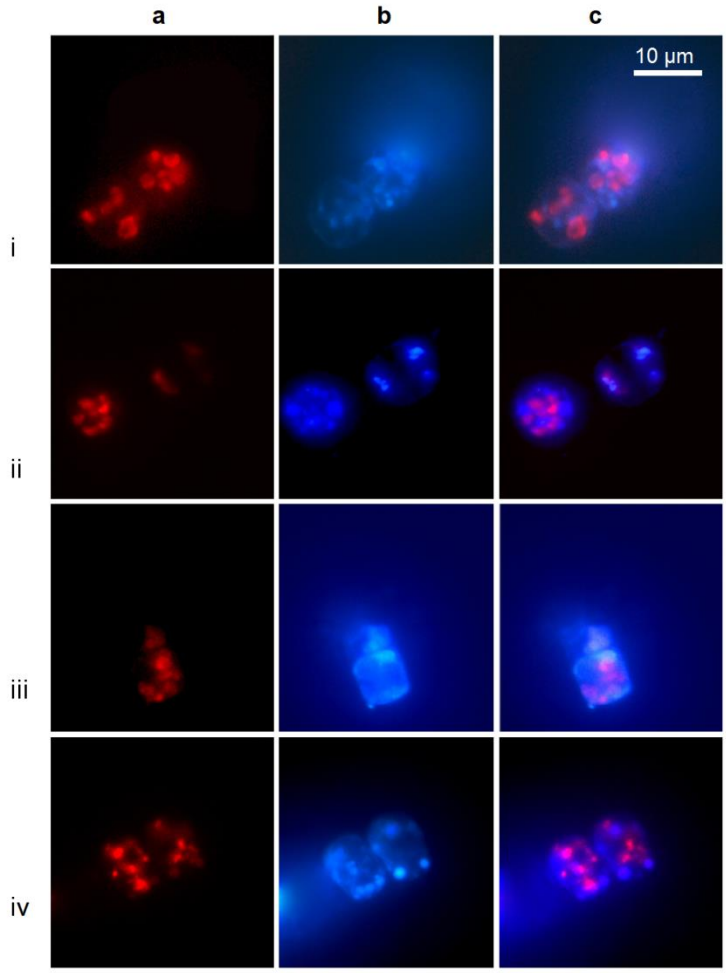


**Figure 2.** Fluorescence microscopy of living *Thalassiosira weissflogii* diatoms stained with PE-Syl. Images recorded with dual-channel settings: a) TRITC-filter set ($\lambda_{exc}$=546 nm, $\lambda_{emi}$=590 nm); b) DAPI-filter set ($\lambda_{exc}$=365 nm, $\lambda_{emi}$=445 nm); c) merge-mode. Images recorded at i: 30 min; ii: 90 min; iii: 8 h; iv: 24 h.

No significant toxic effect of PE-Syl on diatom viability was observed when monitoring the cell density by a Burker haemocytometer immediately after addition (time=0) and at time intervals of 24 h until the measured density reached a plateau value, observed 96 h after the inoculation of the dye (Supporting S3).

The *in vivo* staining was also investigated by flow cytometry, giving real time evidence of the magnitude of the dye's incorporation in an entire population of living diatoms. Flow cytometry allows to detect the enhancement over time solely of blue photoluminescence from PE-Syl stained living cells, excluding any response from dead cells, molecular free dye and possible aggregates present in the investigated medium. Bare cells were analysed to set

scattering and fluorescence thresholds as the parameters that define a living cell population exhibiting only bright red fluorescence due to the chloroplasts. As reported more in detail in the Supporting S4, a significant increase in average blue fluorescence intensity with 70% staining of the cell population was observed immediately after the addition of the dye and, after 4h incubation, the percentage of stained cells in the cell population reached 93%. Such a fast staining response was probably due to the hydrophobicity of PE-Syl which favoured the uptake of the dye molecules by the cell membrane and other internal compartments. Although we have not conclusive experimental proofs, we can suppose that the dye molecules are likely hydrolized and conveyed inside the silica deposition vescicle of diatoms, where the biosilicification process occurs. Here the dye molecules are possibly co-condensed with orthosilicic acid, and covalently anchored to the biomineralized silica network, according to the hypotetic incorporation mechanism reported in the literature for other non emitting alkoxysilane molecules.[17]

**2.2. Purification of the stained biosilica**

Three different protocols from the literature were tested and compared to remove the organic biological matter from the stained biosilica, based on (a) acidic treatment with chloridric acid and methanol (HCl/MeOH, Method A, slightly modified from the literature),[17] (b) sodium dodecyl sulfate and ethylenediaminetetraacetic acid (SDS/EDTA, Method B),[18] (c) sulfuric acid, chloridric acid and hydrogen peroxide ($H_2SO_4$/HCl/$H_2O_2$, Method C),[7a, 19] respectively. The last and most harsh protocol included an oxidative step with $H_2O_2$ to complete protoplasm degradation. Biosilica samples recovered after the cleaning procedures, as well as a reference sample of living diatoms stained with PE-Syl, were analyzed by confocal microscopy (Figure S5).

Methods A and B proved to be unsuitable for the full removal of the organic protoplasm, as shown by the presence of the red photoluminescence of chloroplasts together with the intense blue emission of PE-Syl dispersed in the organic matter inside the cells (Figure S5, lines b and c). Conversely, Protocol C completely removed the protoplasm organic matter including the chloroplasts, as shown by the confocal microscopy images displaying valves with only blue emission (Figure S5, line d).

### 2.3. Morphology and composition of PE-Syl stained biosilica

As observed by SEM microscopy, biosilica obtained by the acidic-oxidative Method C consists mainly of nanostructured valves, similar to "coins" with "milled" edges and cylindrical girdles (Figure 3). Nanopores on both valve and girdle surfaces were not clogged and their pore patterns were preserved after the purification protocol.

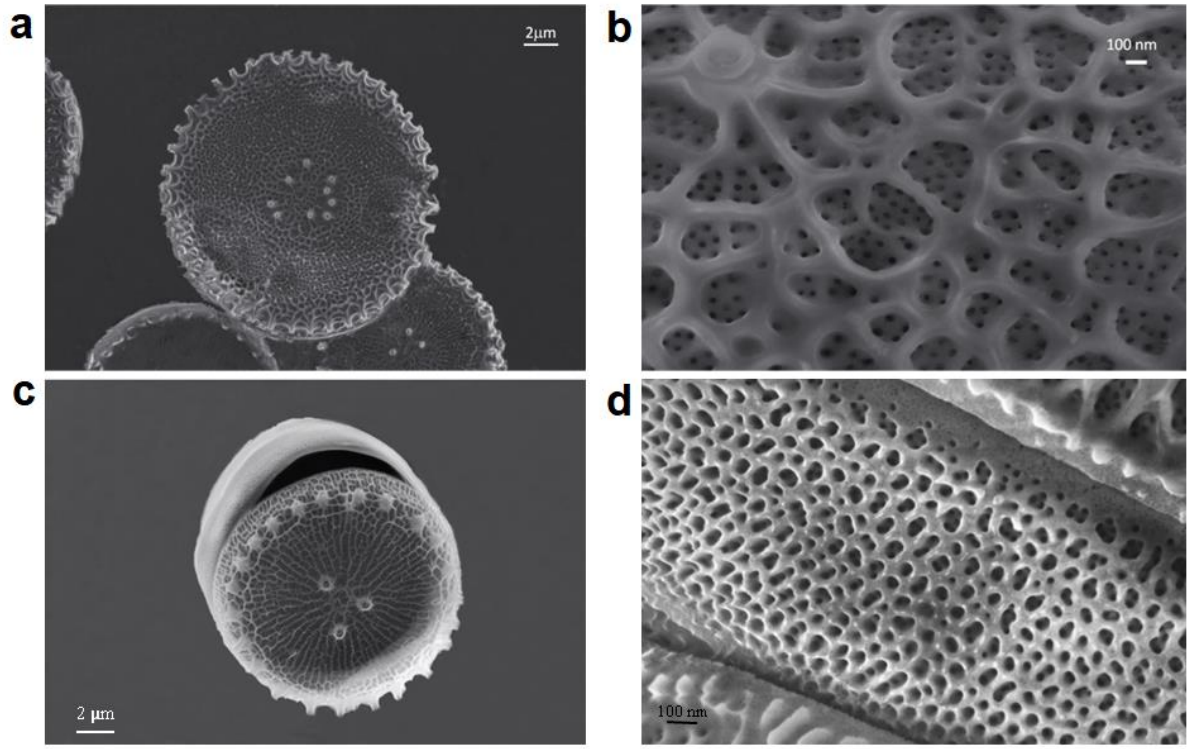


**Figure 3.** SEM images of *Thalassiosira weissflogii* biosilica isolated by Method C: a) full view of the valve; b) valve hierarchical nanostructure; c) valve superimposed on a girdle; d) girdle nanostructure.

3D confocal microscopy reconstruction also revealed the integrity of the valves with a "coin-like milled edge" structure. The photoluminescence of the stained valves was significantly enhanced compared to bare biosilica autofluorescence with almost homogeneous inclusion of the dye throughout the entire valve. A slightly higher concentration at the edges was observed in confocal reconstructions using top and bottom views (Figure 4).

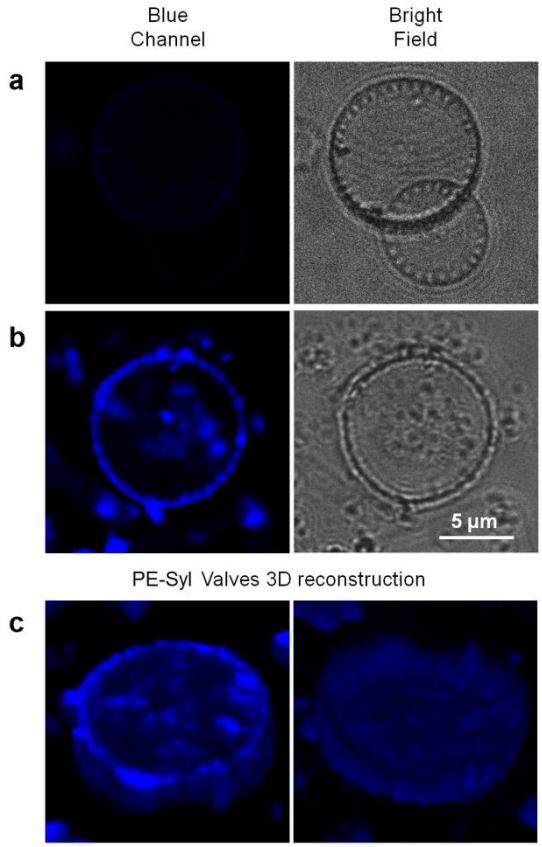


**Figure 4.** Confocal microscopy images in blue channel (left) and bright field (right) of (a) bare valve and (b) PE-Syl stained valve after purification with Method C. (c) 3D confocal reconstruction from the top (left panel) and the bottom (right panel) faces of a PE-Syl stained valve.

Investigation into the stained biosilica composition carried out using Raman, ToF-SIMS and FT-IR spectroscopies demonstrated that cleaning Method C did not damage the PE-Syl structure. Figure 5a compares the Raman spectra for PE-Syl, PE-acid and PE-amide, with those recorded for both bare and PE-Syl functionalized biosilica. The strongest peaks in the Raman spectrum – corresponding to the benzene ring in-plane modes (at 1090 and 1600 $cm^{-1}$) and ethynylene stretching (2207 $cm^{-1}$)[20] – were easily recognizable in all the compounds

despite the strong fluorescent baseline observed for both PE-Syl and PE-acid. The Raman fingerprint for PE-Syl was present in the spectrum of the PE-Syl treated diatoms, while its typical peaks were not present in the spectrum for non-functionalized diatom biosilica. Moreover, intensity mapping of the ethynylene stretching peak in a glass slide coated with PE-Syl-treated biosilica (Figure 5b) revealed non-homogeneous distribution of the dye. In particular, the size of regions with high-signal intensity matched up well with the valves' size, thus confirming the presence of the dye inside the frustule-derived biosilica structures. The sample spectrum, taken at one of the highest intensity regions (see arrow in Figure 5c), is very similar to the PE-amide spectrum, which is a major proof of the fact that the dye preserves its molecular structure after the purification process.

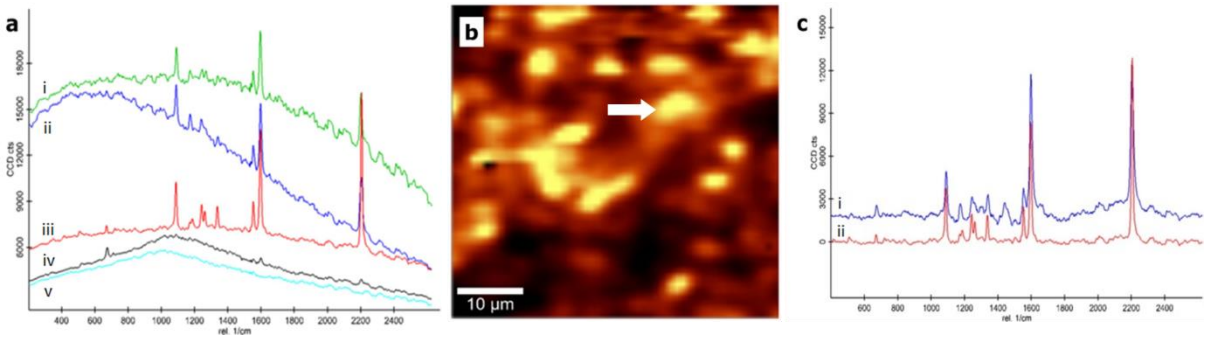


**Figure 5.** a) Raman spectra for (i) PE-Syl, (ii) PE-acid, (iii) PE-amide, (iv) PE-Syl treated diatoms and (v) non-functionalized diatoms. b) Intensity map of the Raman 2207 $cm^{-1}$ signal collected on a 50 µm x 50 µm area in PE-Syl functionalized biosilica sample. Lower intensity regions are darker, higher intensity regions are brighter on the map. c) Baseline subtracted (normalised and y shifted) Raman spectrum at (i) the position labelled with a white arrow in the map b), compared to (ii) the baseline subtracted and normalised spectrum of PE-amide.

FT-IR spectra (Supporting S6) of stained and bare biosilica also confirmed the dye's incorporation with the presence of the C=O stretching (1710 $cm^{-1}$) and N-H bending (1598 $cm^{-1}$) signals of the PE-Syl amide moiety in the sole spectrum of stained shells. Moreover, Si-O (1206 $cm^{-1}$), Si-O-C (1134 $cm^{-1}$) and Si-C stretching signals (1020 $cm^{-1}$) were more intense in the stained biosilica spectrum than in the non-functionalized biosilica spectrum.

Further evidence that the dye's molecular structure survived silica-cleaning protocols came from the ToF-SIMS spectra, though their interpretation is somewhat challenging. As reported

in detail in the Supporting S7, by comparison of specific portions of negative spectra of the bare and the dye stained shells, an increase in the $CHO^-$ peak at 29 m/z (Figure S7b) after the staining of the shells may be accounted as an indication of the possible presence of the incorporated dye. Additional peaks at 60 m/z (Figure S7c) attributable to $SiCH_4O^-$ moieties and at 116 m/z (Figure S7d), are also observed in the dye stained biosilica and in the PE-acid reference samples, as another possible proof of the presence of the dye in the stained silica. Positive spectra of the stained silica and the PE-acid sample also show a similarity of peaks at 204 and 203 m/z probably related to $C_xO_yH_z$ kind of fragmentation (Figure S7e).

### 2.4. Light transmission measurements

A sample of pristine living *Thalassiosira weissflogii* diatoms was subjected to the acidic-oxidative Method C. Light transmission of the resulting structures was recorded by mapping the structures of bare isolated valves and girdles with a single wavelength scan. The resulting valve and girdle transmission maps are shown as insets in Figures 6a,b and 6c, respectively. The light blue crown observed in the valve map relates to the region where transmission of light is lower, as the result of the higher thickness of the circular peripheral edge. Transmission spectra were also recorded at specific points on the maps. Figures 6a and 6b show the valve's transmission spectra in 500 nm spot regions with a predominant contribution of the edge and central nanostructure (arrows in the insets).

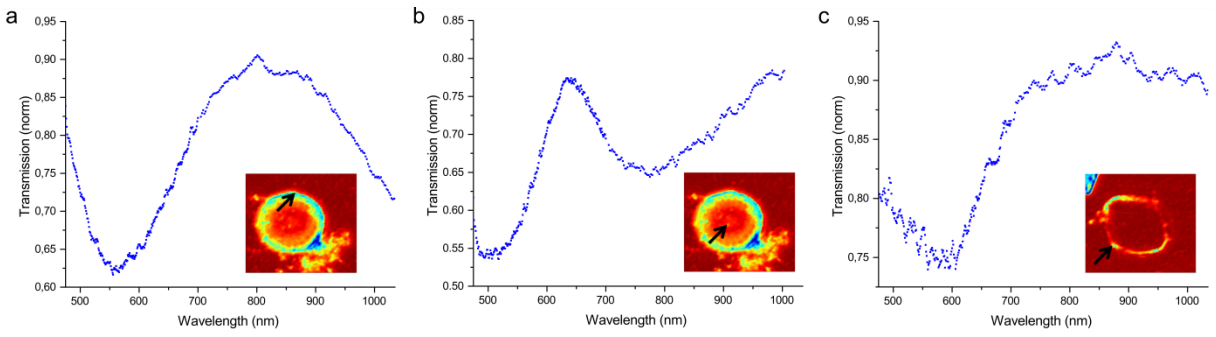


**Figure 6.** Light transmission spectra of a diatom valve in regions with predominant contribution of (a) the edge and (b) the central nanostructure. (c) Light transmission spectrum of a girdle. Insets: Light transmission maps (vertical polarization with respect to the image) of (a, b) a valve and (c) a girdle. The measurement was performed at 550 nm.

The spectra are different and remarkably, in spite of their very similar composition, show features not related to the absorption band of the material. Both observations suggest that the structural colour is emerging due to the biosilica structures' periodic architecture. A transmission depth around 550 nm with a full width at half maximum (FWHM) of about 100 nm observed in the edge region (Figure 6a) can be ascribed to diffraction within the natural grating made by the periodic alternation of air and biosilica, which is responsible for the refractive index periodicity typical of photonic band gap materials. Accordingly, we assign the depth at 550 nm to the photonic band gap of the diatom edge. Moving to the central region (Figure 6b), the two transmission minima suggest a more complex mesoporous nanostructure with a hierarchical distribution of pore patterns in the superimposed periodic structure of the two biosilica layers. Moreover, the transmittance modulation depth is lower than that observed for the edge and girdle, due to the thinner nature of the valve's central portion. The transmission spectrum in one spot on the girdle (Figure 6c, arrow in the inset map) is similar to that reported in Figure 8a for the edge, suggesting that the photonic structure is similar here to that of the edge but with a slightly different periodicity.

A simulation of the optical properties of *Thalassiosira weissflogii* valves was performed using the transfer matrix method (see S8).[21] In particular, the complex three-dimensional system of the diatom valve, with different periodicities of silica and air, was studied using an effective one dimensional model which simplifies the modulation of the refractive index in one dimension considering different lattice pitches. These simplified simulations strongly highlight the photonic behaviour of the diatom valve. The different band gaps seen in the experimental data are explained by different periodicities of silica and air in both valve edge and valve centre (see details in S8).

**2.5. Photoluminescence measurements**

Figure 7a (green line) shows the photoluminescence spectrum of a thin film of PE-Syl stained biosilica (purified by Method C) casted from a chloroform suspension on a glass slide and thermally annealed at 70 °C. The emission spectrum of a film of pure PE-Syl drop-casted from a chloroform solution is also reported (Figure 7a, red line). The two spectra are vastly different. The emission spectrum of PE-Syl incorporated in the biosilica peaks at 580-590 nm while the emission peak of the neat dye in the thin film peaks at 500 nm.

Photoluminescence of the stained biosilica was also compared to the emission spectra of (i) a standard glass slide (grey curve in Figure 7b), (ii) a film of bare biosilica isolated from living diatoms by Method C (black curve), (iii) a film of the same isolated biosilica after surface functionalizion with PE-Syl molecules by covalent condensation reaction of the trietoxysilyl group of the PE-Syl dye (dark green curve) and (iv) a film obtained by drop casting the product of the acidic-oxidative procedure (as in Method C) performed on a solution of PE-Syl (brown curve, Figure 7b).

The following considerations may be drawn when comparing the spectra: 1) the emission spectrum of the biosilica after the *in vivo* feeding with PE-Syl and acidic-oxidative treatment (bulk stained biosilica) is clearly different from the autofluorescence of bare biosilica and glass; 2) the emission profile of PE-Syl covalently attached on the biosilica surface is very similar to that of the neat PE-Syl film and only weakly affected by the periodic nanostructure, differing mainly in the presence of a shoulder at 580 nm in the surface stained biosilica spectrum (dark green in Figure 7b). 3) On the contrary, the shape of the spectrum of PE-Syl incorporated in the biosilica (light green line in Figures 7a and 7b) shows that the dye's photoluminescence is strongly modulated by the valve's photonic structure. In fact, the light transmission peak in the valve's central region (blue line in Figure 7a), which represents the largest portion of the biosilica exposed to excitation in thin film, is exactly positioned where the peak of the PE-Syl stained biosilica emission is revealed. Overall, *the PE-Syl bulk stained*

*biosilica shows a filtered emission, due to the waveguide interaction between the periodic structure of the biosilica and the dye*;[22] 4) the observation that the emission of pure PE-Syl has totally dropped out as a result of the acidic-oxidative protocol, as a consequence of the dye degradation, combined with the FTIR and ToF-SIMS evidence discussed above of the structural integrity of the PE-Syl molecules in the silica shells, indicates that *the PE-molecule is deeply embedded into the biosilica which acts as a protecting and confining environment for the dye in the stained structures, preventing its degradation*.

Emission measurements as a function of the detection angle were also performed (Supporting, Fig.S9). By increasing the angle with respect to a direction orthogonal to the valve structure, a shift of a few nanometers (less than the one expected for a pure single pitch photonic structure) in the emission peak was observed, probably due to the variation in the diatom's complex photonic band gap structure.

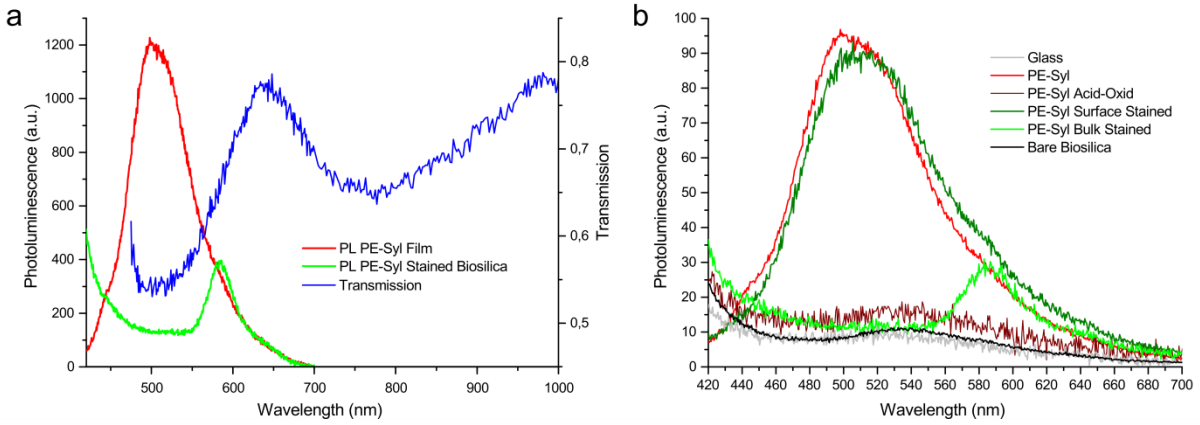


**Figure 7.** (a) Emission spectra of PE-Syl dye (red) and PE-Syl stained biosilica (light green), together with characteristic transmission spectra of the valve centre (blue). (b) Comparison of emission spectra of: glass (grey), PE-Syl dye (red), PE-Syl after acid-oxidative treatment (brown), PE-Syl covalently attached to the biosilica surface (dark green), bare biosilica (black), dye bulk stained biosilica (light green).

### 2.6. Spatially resolved analysis by confocal microscopy

A spatially resolved study of photoluminescence in specific regions of the PE-Syl stained biosilica was carried out by confocal microscopy. Individual objects consisting of a girdle still

attached to a valve were selected in the biosilica sample obtained from the acidic-oxidative cleaning procedure of stained diatoms.

Three different regions of interest were considered, namely the edge, the central nanostructure and the girdle (Figure 8). Two fluorescence emission spectra were recorded in a few $\mu m^2$ spots for each region of four biosilica objects. The eight collected spectra per region were averaged giving three different emission profiles (spotted line) with their average tendency line (continuous line) with a mobility factor of 3. Comparison of photoluminescence in the selected regions (*i.e.* edge, girdle and central valve nanostructure) highlights a similarity in the emission spectra of the edge and girdle, showing a peak around 535-540 nm. Conversely, as the result of the different substructure lattice of the girdle and edge versus the central nanostructure, photoluminescence recorded in the central region of the valve was about 50 nm red-shifted, peaking at around 585 nm.

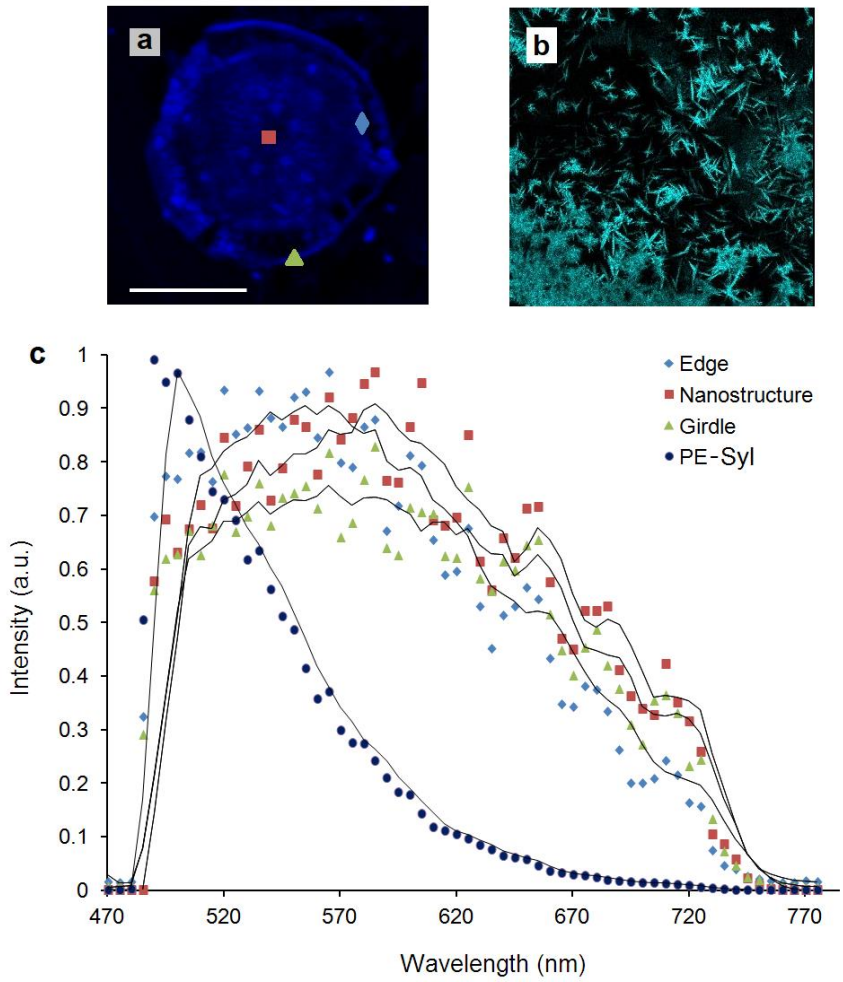


**Figure 8.** a) Confocal image of a structure containing valve (red square), edge (chamber rhombus) and girdle (green triangle) substructures from cleaned frustules after feeding *Thalassiosira weissflogii* diatoms with PE-Syl (marker: 5 µm). b) PE-Syl deposited in a solid state on a glass slide. c) Photoluminescence spectra of the three lattice substructures and solid PE-Syl.

## 3. Conclusion

In this paper, we have followed in the footsteps of others who have used staining to investigate diatoms' life cycles but, changing perspective, we have pursued generation of hybrid photonic structures from frustules. Specifically, we have shown that *in vivo* staining with appropriate dyes provides a valuable way to study the intimate photonic properties of the natural architecture of diatom frustules. Detailed analysis based on fluorescence and confocal microscopies in combination with transmission and emission spectroscopies has demonstrated that, when adopting the proposed procedure, the dye is homogeneously dispersed throughout

the biosilica and that modulation of the dye's photoluminescence is induced by the valves' and girdles' photonic crystal structures.

Essentially, hybrid biophotonic nanostructures have been created whose optical properties derive from the interaction of the photonic properties of the nanostructured silica shells of *Thalassiosira weissflogii* diatoms with those of the tailored molecular fluorophores. Most significantly, the diatom shells' valves and girdles retain their natural periodic nanostructures when the fluorescent biosilica micro/nano structures are isolated from the living algae by acidic-oxidative treatment. Thanks to the dye's deep-down penetration and its incorporation into the very core of the biosilica shell, a process which allocates and protects the dye – and which thus goes well beyond mere *a posteriori* functionalization of the algae backbone – a further instrument has been added to the research toolkit.

How can this tool be used? Various further steps can be foreseen. Possible applications include light filtering and trapping for energy harvesting. Moreover, light management by the biosilica photonic crystal may generate a natural resonant cavity for random lasing by optically pumping a suitable active dye into the structure which may, in turn, lead to local metrology that allows the structure to be further characterised.

## 4. Experimental Section

*In vivo staining*: A sample of 500 µL from the diatoms' culture was diluted with 5 mL of commercial Guillard's solution enriched with glucose (5.6 $\mu gL^{-1}$) and sodium metasilicate (30 $mgL^{-1}$). Subsequently, a DMSO solution (120 µL) of PE-Syl (2.2 mg, 0.03 M) was added to 5 mL of sterile sodium-metasilicate free sea water. This staining solution was filtered (0.2 µm) and mixed to the cell medium mentioned above. The final flask density was $4 \cdot 10^5$ diatoms $mL^{-1}$. Hence, the final PE-Syl concentration was 0.33 mM. Kanamycin was used at a final concentration of 50 $\mu gL^{-1}$ to avoid bacterial contamination. The staining process was performed over four days, gently stirring the cell medium (stirring rate < 100 rpm).

*Microscopy*: Bidimensional fluorescence images of living diatoms and dye functionalized biosilica were recorded using an Axiomat microscope, Zeiss (German). SEM analysis was performed with a Philips XL 20 scanning electron microscope (FEI, Milan, Italy). For photophysical and morphological characterization, a confocal laser scanning microscope Leica SP8 X with upright configuration, was also used: 3D and λ scan images were performed using a UV/Diode laser with 405 nm excitation wavelength and an HC PL APO CS2 63x/1.40 Oil objective. Emission spectra were recorded in the 420-780 nm spectral range. This interval was divided into 72 detection steps with a 5 nm stepsize.

*Comparison of different purification methods of luminescent biosilica*: *In vivo* staining was carried out, as previously described, on a set of four equivalent samples (500 µL) of diatom culture. After staining, cells were collected by soft centrifugation (1300 rpm, 15 min) and rinsed with doubly distilled water (total volume 400 µL). One resulting sample was used as a blank while the others were subjected to the following purification methods.

*Method A*: According to the procedure reported by Lang *et al.*[17] cells were suspended in HCl (300 µL, 36% v/v) and the system was wept overnight without stirring to allow sedimentation. Distilled water (200 µL) was then added and the supernatant was removed after centrifugation at 1300 rpm for 15 minutes. The precipitate was washed with methanol (500 µL) and, after centrifugation and removal of the solvent, the entire procedure described in Method A was repeated three times.

*Method B*: As reported by Poulsen *et al.*,[18] the stained cells were suspended in SDS solution (200 µL, 4% v/v), and 200 µL of aqueous EDTA 0.2M were added. The mixture was heated to reflux for five minutes and kept overnight at room temperature without stirring to allow sedimentation. Distilled water (200 µL) was then added and the supernatant was removed after centrifugation (1300 rpm, 15 min). The precipitate was finally double-washed with distilled water (2x200 µL).

*Method C*: The stained cells were suspended in a mixture of $H_2SO_4$ (150 µL, 98% w/w) and HCl (100 µL, 4N) at 70 °C for 10 min. A further oxidation step was carried out adding $H_2O_2$ (300 µL, 30% w/w) and heating to 90 °C for 4 h. The biosilica was finally recovered after four washings with distilled water (4x200 µL) and soft centrifugation (1300 rpm, 15 min). This method was adapted and optimized from the literature.[7a]

*Raman spectroscopy*: Raman spectroscopic analysis of the samples was performed in dry state without further modification, using a WITec alpha300 confocal Raman microscope at 633 nm excitation wavelength. Raman spectra were collected with a 10x objective at 2 s accumulation time and 10 measurements were averaged to compare the spectra of the various PE-derivatives with the spectra of functionalised PE-Syl and bare biosilica under similar conditions without smoothing or baseline subtraction. The 2D map of the functionalized biosilica sample was generated using the WITec Project software based on spectra collected for 10 s at 1 µm resolution covering a 50 µm x 50 µm area and calculating the integrated signal intensity of the peak at 2207 $cm^{-1}$ Raman shift for each pixel after baseline subtraction.

*Light Transmission analysis*: The set-up consisted of a microscope in transmission configuration. The probe light came from a NKT Photonics SuperK Select laser, continuously tunable from 475 to 1050 nm. The transmitted light was detected with an optical fibre connected to a silicon-based photodiode. Light transmission was spatially resolved by raster-scanning the sample with respect to the laser beam through a piezo stage (P-517 Physik Instrumente) on the x-y plane, with the z excursion used to optimize the focus on the sample. Transmittance was calculated as $T=I/I_0$ by recording $I_0$ in a region without diatoms, and I in a region with diatoms.

*Photoluminescence analysis set-up*: The photoluminescence measurement was performed with a CW diode laser at 375 nm, focused on the sample with a circular lens (focal length 100 mm). Emitted light was collected with a fibre bundle tilted with different angles with respect

to the sample orthogonal direction. Luminescence was detected with a cooled spectrometer (Princeton Instruments). The laser's spot diameter was about 200 μm.

**Supporting Information**
Supporting Information is available from the Wiley Online Library or from the author.

**Acknowledgements**

This work was financed by Università degli Studi di Bari "Aldo Moro" (IDEA Giovani Ricercatori 2011 project: "BIOEXTEND: Extending enzymatic properties by bioconjugation of enzymes with fluorescent organic oligomers") and by the Ministero dell'Istruzione dell'Università e della Ricerca (MIUR) (PON02_00563_3316357 project "Materials Nanotechnology for Health and Environment" MAAT). Thanks go to Prof. Anthony Baldry, University of Messina, for consultation over the drafting of the final version and to Dr. Vita Pinto for contribution to the dyes' synthesis.

Received: ((will be filled in by the editorial staff))
Revised: ((will be filled in by the editorial staff))
Published online: ((will be filled in by the editorial staff))

**References**

[1] a) J. Seckbach, J. P. Kociolek, *The Diatom World*, Springer, Netherlands, 2011; b) R. Wetherbee, *Science* **2002**, 298, 547; c) F. E. Round, R. M. Crawford, D. G. Mann, *The Diatoms*, Cambridge University Press, Cambridge, UK, 1990.

[2] M. Hildebrand, S. J. L. Lerch, *Seminars in Cell & Developmental Biology* **2015**, *46*, 27.

[3] a) S. W. Fowler, N. S. Fisher, *Deep-Sea Res. Part A* **1983**, *30*, 963; b) C. E. Hamm, R. Merkel, O. Springer, P. Jurkojc, C. Maier, K. Prechtel, V. Smetacek, *Nature* **2003**, *421*, 841: c) J. A. Raven, A. M. Waite, *New Phytol.* **2004**, *162*, 45.

[4] a) M. S. Hale, J. G. Mitchell, *Aquat. Microb. Ecol.* **2001**, *24*, 287; b) A. J. Milligan, F. M. M. Morel, *Science* **2002**, *297*, 1848.

[5] a) R. Gordon, D. Losic, M. A. Tiffany, S. S. Nagy, F. A. S. Sterrenburg, *Trends Biotechnol*. **2009**, *27*, 116; b) A. T. Davidson, D. Bramich, H. J. Marchant, A. McMinn, *Mar. Biol.* **1994**, *119*, 507; c) E. De Tommasi, I. Rea, V. Mocella, L. Moretti, M. De Stefano, I. Rendina, L. De Stefano, *Opt. Express* **2010**, *18*, 12203.

[6] a) J. E. N. Dolatabadi, M. de la Guardia, *Trends in Analytical Chemistry* **2011**, *30*, 1538; b) I. Rea, M. Terracciano, L. De Stefano, *Adv. Healthcare Mater.* **2017**, *6*, 1601125.

[7] a) S. R. Cicco, D. Vona, E. De Giglio, S. Cometa, M. Mattioli-Belmonte, F. Palumbo, R. Ragni, G. M. Farinola, *ChemPlusChem* **2015**, *80*, 1104; b) B. Delalat, V. C. Sheppard, S. Rasi Ghaemi, S. Rao, C. A. Prestidge, G. McPhee, M.-L. Rogers, J. F. Donoghue, V. Pillay, T. G. Johns, N. Kroger, N. H. Voelcker, *Nat. Commun*. **2015**, *6*, 8791.

[8] a) C. Jeffryes, J. Campbell, H. Li, J. Jiao, G. Rorrer, *Energy Environ. Sci.* **2011**, *4*, 3930; b) X. W. Sun, Y. X. Zhang, D. Losic, *J. Mater. Chem. A* **2017**,*5*, 8847; c) K. H. Sandhage, S. M. Allan, M. B. Dickerson, C. S. Gaddis, S. Shian, M. R. Weatherspoon, Y. Cai, G. Ahmad, M. S. Haluska, R. L. Snyder, *Int. J. Appl. Ceram. Technol.* **2005**, *2*, 317; d) K. H. Sandhage, M. B. Dickerson, P. M. Huseman, M. A. Caranna, J. D. Clifton, T. A. Bull, T. J. Heibel, W. R. Overton, M. E. A. Schoenwaelder, *Adv. Mater*. **2002**, *14*, 429; e) Z. Bao, R. M. Weatherspoon, S. Shian, Y. Cai, P. D. Graham, S. M. Allan, G. Ahmad, M. B. Dickerson, B. C. Church, Z. Kang, H. W. Abernathy III, C. J. Summers, M. Liu, K. H. Sandhage, *Nature* **2007**, *446*, 172; f) R. R. Unocic, F. M. Zalar, P. M. Sarosi, Y. Cai, K. H. Sandhage, *Chem.Commun.* **2004**, 796.

[9] a) R. Ragni, S. Cicco, D. Vona, G. Leone, G. M. Farinola, *J. Mater. Res.* **2017**, *32*, 279; b) R. Ragni, S. R. Cicco, D. Vona, G. M. Farinola, *Adv. Mater.*, DOI:10.1002/adma.201700593; c) R. Ragni, S. R. Cicco, D. Vona, G. M. Farinola, in *Green Materials for Electronics*, (Eds. M. Irimia-Vladu, E. Glowacki, N. S. Sariciftci, S. Bauer, Wiley-VCH Verlag GmbH & Co.

KGaA, Boschstr 12, 69469, Weinheim, Germany, **2018**, Ch.11; d) E. De Tommasi, *Journal of Spectroscopy* **2016**, 2490128/1.

[10] a) T. Fuhrmann, S. Landwehr, M. El Rharbi-Kucki, M. Sumper, *Applied Physics B* **2004**, *78*, 257; b) M. A. Ferrara, P. Dardano, L. De Stefano, I. Rea, G. Coppola, I. Rendina, R. Congestri, A. Antonucci, M. De Stefano, E. De Tommasi, *PLoS One* **2014**, *9*, e103750; c) L . De Stefano, I. Rea, I. Rendina, M. De Stefano, L. Moretti, *Optics Express* **2007**, *15*,18082. d) K. Kieu, C. Li, Y. Fang, G. Cohoon, O. D. Herrera, M. Hildebrand, K. H. Sandhage, R. A. Norwood, *Optic Express* **2014**, *22*, 15992.

[11] a) J. Desclés, M. Vartanian, A. El Harrak, M. Quinet, N. Bremond, G. Sapriel, J. Bibette, P. L. Lopez, *New Phytologist* **2008**, *177*, 822; b) V. V. Annenkov, E. N. Danilovtseva, S. N. Zelinskiy, T. N. Basharina, T. A. Safonova, E. S. Korneva, Y. V. Likhoshway, M. A. Grachev, *Anal. Biochem.* **2010**, *407*, 44.

[12] M. Kucki, T. Fuhrmann-Lieker, *J. R. Soc. Interface* **2012**, *9*, 727.

[13] A. Operamolla, R. Ragni, O. Hassan Omar, G. Iacobellis, A. Cardone, F. Babudri, G. M. Farinola, *Curr. Org. Synth.* **2012**, *9*, 764.

[14] A. Cardone, F. Lopez, F. Affortunato, G. Busco, A. M. Hofer, R. Mallamaci, C. Martinelli, M. Colella, G. M. Farinola, *Biochimica et Biophysica Acta* **2012**, *1818*, 2808.

[15] a) F. Milano, R. R. Tangorra, O. Hassan Omar, R. Ragni, A. Operamolla, A. Agostiano, G. M. Farinola, M. Trotta, *Angew. Chem. Int. Ed.* **2012**, *51*, 11019; b) O. Hassan Omar, S. la Gatta, R. R. Tangorra, F. Milano, R. Ragni, A. Operamolla, R. Argazzi, C. Chiorboli, A. Agostiano, M. Trotta, G. M. Farinola, *Bioconjugate Chem.* **2016**, *27*, 1614; c) A. Operamolla, R. Ragni, F. Milano, R. R. Tangorra, A. Antonucci, A. Agostiano, M. Trotta, G. M. Farinola, *J. Mater. Chem. C* **2015**, *3*, 6471; d) S. la Gatta, O. Hassan Omar, A. Agostiano, F. Milano, R. R. Tangorra, A. Operamolla, C. Chiorboli, R. Argazzi, M. Trotta, G. M. Farinola, R. Ragni *MRS Advances* **2016**, *1(7)*, 495.

[16] a) D. J. Belton, O. Deschaume, C. C. Perry, *FEBS J.* **2012**, *279*, 1710; b) N. Kröger, R. Deutzmann, M. Sumper, *Science* **1999**, *286*, 1129; c) N. Kröger, R. Deutzmann, C. Bergsdorf, M. Sumper, *PNAS* **2000**, *97*, 14133.

[17] Y. Lang, F. del Monte, L. Collins, B. J. Rodriguez, K. Thompson, P. Dockery, D. P. Finn, A. Pandit, *Nature Commun*. **2013**, *4*, 2683.

[18] N. Poulsen, N. Kröger, *J. Biol. Chem.* **2004**, *279*, 42993.

[19] a) D. Vona, L. Urbano, M. A. Bonifacio, E. De Giglio, S. Cometa, M. Mattioli-Belmonte, F. Palumbo, R. Ragni, S. R. Cicco, G. M. Farinola, *Data in Brief* **2016**, *8*, 312; b) S. R. Cicco, D. Vona, G. Leone, M. Lo Presti, F. Palumbo, E. Altamura, R. Ragni, G. M. Farinola, *MRS Commun.* **2017**, *7*, 214; c) D. Vona, M. Lo Presti, S. R. Cicco, F. Palumbo, R. Ragni, G. M. Farinola, *MRS Advances* **2016**, *1(57)*, 3817.

[20] Z. Liu, X. Wang, K. Dai, S. Jin, Z.-C. Zeng, M.-D. Zhuang, Z.-L. Yang, D.-Y. Wu, B. Ren, Z.-Q. Tian, *J. Raman Spectrosc.* **2009**, *40*, 1400.

[21] M. Born, E. Wolf, *Principles of Optics: Electromagnetic Theory of Propagation, Interference and Diffraction of Light*, Cambridge University Press, **2000**.

[22] C. Jeffryes, R. Solanki, Y. Rangineni, W. Wang, C-H. Chang, G. L. Rorrer, *Adv. Ma*ter. **2008**, *20*, 2633.

**Table of contents entry:**

The *in vivo* incorporation of a tailored organic fluorophore into diatom algae is a promising route to hybrid materials with properties resulting from the combination of the fluorophore luminescence and the photonic nanostructure of biosilica shells of diatoms

**Keywords: photonic crystals, diatoms, biosilica, photoluminescence, molecular emitters**

Roberta Ragni, Francesco Scotognella, Danilo Vona, Luca Moretti, Emiliano Altamura, Giacomo Ceccone, Dora Mehn, Stefania R. Cicco, Fabio Palumbo, Guglielmo Lanzani* and Gianluca M. Farinola*

**Hybrid photonic nanostructures by in vivo incorporation of an organic fluorophore into diatom algae**